

NASA/CR-80-

208066

NASA-16263-701

N15

Reprinted from

71-11-12

*JOURNAL OF QUANTITATIVE SPECTROSCOPY AND
RADIATIVE TRANSFER*

Vol. 23, No. 2, pp. 221-227

**BAND MODEL CALCULATIONS FOR CFCl_3 IN
THE $8\text{-}12\mu\text{m}$ REGION**

PETER M. SILVAGGIO and ROBERT W. BOESE

NASA-Ames Research Center, Moffett Field, CA 94035, U.S.A.

and

ROGER NANES

Department of Physics, California State University, Fullerton, CA 92634, U.S.A.

PERGAMON PRESS

NEW YORK · OXFORD · TORONTO · PARIS
FRANKFURT · SYDNEY

1980

BAND MODEL CALCULATIONS FOR CFCI_3 IN THE $8-12 \mu\text{m}$ REGION

PETER M. SILVAGGIO[†] and ROBERT W. BOESE
NASA-Ames Research Center, Moffett Field, CA 94035, U.S.A.

and

ROGER NANES[‡]
Department of Physics, California State University, Fullerton, CA 92634, U.S.A.

(Received 6 June 1979)

Abstract—A Goody random band model with a Voigt line profile is used to calculate the band absorption of CFCI_3 at various pressures at room and stratospheric (216°K) temperatures. Absorption coefficients and line spacings are computed.

I. INTRODUCTION

The vibration-rotation bands of freon 11 (CFCI_3) have been studied in the past.¹⁻⁵ This heavy symmetric top molecule with very small rotational constants has a multitude of rotational lines in the bands near $10 \mu\text{m}$, which should explain the lack of any discernable rotational structure at modest resolution. Thus, the spectral absorption coefficients for trichloro-fluoromethane should be a slowly varying function of wavelength, making it an ideal candidate for a band model analysis.

2. THEORETICAL CONSIDERATIONS

The general theory of the random band model was first developed by N. Mayer⁷ and later by Goody⁶ and is only briefly described here. The absorption lines are assumed to be randomly spaced with their intensities distributed according to a Poisson distribution. The wings of the lines in the center of the spectral interval being modeled must have a negligible contribution outside that interval. The general form of the random band model is

$$\bar{T} = \exp \left[-\frac{1}{\delta} \int_{-\infty}^{\infty} \frac{k\rho l \delta f_{\nu}}{1 + k\rho l \delta f_{\nu}} d\nu \right] \quad (1)$$

where ρ is the density (amagat), l is the length (cm), k is the mean absorption coefficient (cm^{-1} amagat $^{-1}$), δ is the mean line spacing (cm^{-1}), and f_{ν} is a line shape function. Over the interval that defines \bar{T} , k , and δ are constant. The integration over the Poisson distribution has already been performed.

For the widest range of utility, the Voigt line shape is the most realistic profile to use for f_{ν} . The appropriate absorption profile can be written (see Penner⁷) as

$$f_{\nu} = \frac{\sqrt{(\ln 2)}}{\alpha_D \sqrt{\pi}} V(x, y) = \frac{\sqrt{(\ln 2)}}{\alpha_D \sqrt{\pi}} \frac{y}{\pi} \int_{-\infty}^{\infty} \frac{\exp(-t^2)}{y^2 + (x - t)^2} dt \quad (2)$$

where

$$y = \left(\frac{\alpha_L}{\alpha_D} \right) \sqrt{(\ln 2)}, \quad x = \left(\frac{\nu - \nu_0}{\alpha_D} \right) \sqrt{(\ln 2)}$$

with α_L and α_D the Lorentz and Doppler halfwidths at halfmaximum, and ν_0 is the frequency of

[†]NAS-NRC Resident Research Associate.

[‡]Supported in part by NASA University Consortium Joint Research Interchange No. NCA2-OR253-701.

the line center. A fast algorithm for the calculation of the Voigt profile is available from Pierlussi *et al.*⁸ The integral in the general equation, Eq. (1), can be expressed as

$$\bar{T} = \exp \left[-\frac{2k\rho l}{\sqrt{\pi}} \int_0^{\infty} \frac{V(x, y) dx}{\left[1 + \frac{k\rho l \delta \sqrt{\ln 2}}{\alpha_D \sqrt{\pi}} V(x, y) \right]} \right]. \quad (3)$$

The Lorentz halfwidth can be expressed as

$$\alpha_L = \alpha_a^0 P_a + \alpha_f^0 P_f, \quad (4)$$

where P_a , P_f are the partial pressures (atm) and α_a^0 , α_f^0 are the pressure broadening coefficients ($\text{cm}^{-1}/\text{atm}$) for the absorber and the foreign gas respectively.

Equation (3) was evaluated by Romberg's numerical integration technique as described by de Boor.¹⁹ The band model was fitted to the laboratory transmission data of Nanes *et al.*⁵ at constant temperature using a least squares fit to a non-linear function with a linearization of the fitting function as described in Bevington.¹⁰ Using this method it is possible to determine the following parameters for a given frequency interval, $\Delta\nu$: k , mean absorption coefficient ($\text{cm}^{-1}/\text{amagat}^{-1}$); δ , mean line spacing (cm^{-1}); α_a^0 , Lorentz self-broadening coefficient ($\text{cm}^{-1}/\text{atm}$); α_f^0 , Lorentz foreign gas broadening coefficient ($\text{cm}^{-1}/\text{atm}$).

The goodness of fit to observations can be measured by the reduced chi square test which can be expressed as

$$\chi^2 = \frac{1}{N_f} \sum_i [\bar{T}_i - \bar{T}(x_i)]^2 \quad (5)$$

where \bar{T}_i is the measured transmission level, $\bar{T}(x_i)$ is the calculated level, and N_f is the number of degrees of freedom (number of spectra - number of parameters being determined).

Using Eq. (5) χ^2 was calculated for given values of k , δ , and α_L^0 . These parameters were then adjusted until χ^2 was minimized. We have selected as our measure of uncertainty in the parameters determined by this technique, the uncertainty that corresponds to an increase of the minimum χ^2 by 100%. That is, if we change one parameter a_m by an amount Δa_m and optimize all the other parameters $a_{i \neq m}$ for a new minimum χ^2 , then the new value of χ^2 will be twice the old value:

$$\chi^2(a_m + \Delta a_m) = 2\chi^2(a_m). \quad (6)$$

The utility of the band model can be extended by applying the following

$$S_v^0 = \int_{\Delta\nu} k_v d\nu \approx \sum_i (k)_i \Delta\nu_i. \quad (7)$$

Thus, once the absorption coefficients have been determined, the band intensity, S_v^0 , may be derived from those parameters of the model.

3. RESULTS

The average transmission for a given interval was calculated from the equivalent width measured by Nanes *et al.*⁵ for that interval. This transmission value along with the experimental conditions of pressure, path length, and temperature formed the data sets for the modeling program. The computed results are presented in Table 1 and displayed in Fig. 1 for both the room ($294 \pm 1^\circ\text{K}$) and the low ($216 \pm 2^\circ\text{K}$) temperature spectra. The four band complexes in the $760\text{--}1120\text{ cm}^{-1}$ region were each modeled at low resolution (a broad interval covering an entire band) and at moderate resolution (intervals spanning 10 cm^{-1}).

If the line shape were Lorentzian, then Eq. (1) can be analytically integrated and a significant amount of computation can be eliminated. Our least squares fitting algorithm failed to converge to any meaningful values when using the Lorentz line shape. Only when the Voigt

Table 1. Band model parameters of the i.r. bands of CFCl_3 (freon 11) in the $8\text{-}12\text{ }\mu\text{m}$ region. The first row of parameters for each interval corresponds to 294°K data, the second row to 216°K data.

Interval cm^{-1}	Chi Sq 10^{-4}	k cm^{-1}	σ milli cm^{-1}	δ milli cm^{-1}	α_L^0 $\text{cm}^{-1}/\text{atm}$	α_L^0 $\text{cm}^{-1}/\text{atm}$	Interval cm^{-1}	Chi Sq 10^{-4}	k cm^{-1}	σ milli cm^{-1}	δ milli cm^{-1}	α_L^0 $\text{cm}^{-1}/\text{atm}$	α_L^0 $\text{cm}^{-1}/\text{atm}$	
760 - 810	0.012	0.49	0.07	7.01	10.61	0.082	870 - 880	0.095	0.14	0.02	1.01	14.35	0.082	
	0.010	0.39	0.08	28.39	28.97	0.102	4.295	0.042	0.07	0.01	2.15	+	0.102	
810 - 880	0.052	26.16	0.31	1.91	0.03	0.082	0.011	910 - 920	0.046	0.22	0.03	11.53	9.79	0.082
	0.541	24.44	1.10	2.20	0.13	0.102	0.039	2.800	0.30	0.11	11.19	+	0.102	
910 - 960	0.017	1.07	0.02	0.62	0.20	0.082	0.408	920 - 930	0.031	1.59	0.01	0.12	+	0.082
	0.068	0.92	0.01	0.10	0.14	0.102	2.533	0.080	1.24	0.01	0.36	+	0.102	
1030 - 1120	0.050	7.52	0.07	1.60	0.03	0.082	0.082	930 - 940	0.201	2.55	0.03	0.19	+	0.082
	0.109	7.43	0.11	1.88	0.05	0.102	0.102	0.158	0.158	2.57	0.02	0.08	+	0.102
770 - 780	0.030	0.22	0.16	73.69	139.80	0.082	940 - 950	0.057	1.11	0.03	0.31	0.35	0.082	0.102
	0.015	0.39	0.69	714.80	597.00	0.102	0.102	0.287	0.97	0.03	0.09	+	0.09	0.102
780 - 790	0.013	0.52	0.01	1.75	28.94 [†]	0.082	950 - 960	0.010	0.08	0.02	29.00	37.42	0.082	0.102
	0.026	0.43	0.13	23.99	28.94	0.102	0.102	0.509	0.02	0.02	3.72	212.20	0.102	0.102
790 - 800	0.026	0.92	0.10	5.37	4.96	0.082	1030 - 1040	0.040	0.10	0.03	20.34	45.87	0.082	0.102
	0.018	0.73	0.09	7.76	6.57	0.102	0.102	0.014	0.13	0.09	404.50	200.80	0.102	0.102
800 - 810	0.022	0.74	0.02	0.41	10.78	0.082	1040 - 1050	0.024	0.31	0.01	0.81	+	0.082	0.102
	0.021	0.62	0.11	12.30	10.78	0.102	0.102	0.015	0.22	0.02	6.96	4.69	0.102	0.102
810 - 820	0.130	1.46	0.03	0.02	0.17	0.082	1050 - 1060	0.043	1.55	0.01	0.19	+	0.082	0.102
	0.054	0.98	0.01	0.01	+	0.102	0.102	0.036	0.61	0.01	0.22	+	0.102	0.102
820 - 830	0.065	4.52	0.04	0.03	0.03	0.082	1060 - 1070	0.062	8.82	0.05	0.11	0.01	0.082	0.102
	0.072	2.05	0.01	0.003	+	0.102	0.102	0.075	5.71	0.05	0.31	0.02	0.102	0.102
830 - 840	0.136	24.68	0.17	0.13	0.01	0.082	1070 - 1080	0.119	18.64	0.11	0.01	0.01	0.082	0.102
	0.137	13.89	0.11	0.22	0.01	0.102	0.102	0.219	19.98	0.17	0.08	0.01	0.082	0.102
840 - 850	0.121	99.06	1.15	0.05	0.01	0.082	1080 - 1090	0.095	23.05	0.13	0.07	0.01	0.082	0.102
	0.806	99.74	1.87	0.11	0.01	0.102	0.102	0.263	25.24	0.23	0.12	0.01	0.082	0.102
850 - 860	0.631	41.06	0.66	0.34	0.02	0.082	1090 - 1100	0.209	9.39	0.05	0.02	+	0.082	0.102
	0.831	45.63	0.87	0.40	0.02	0.102	0.102	0.091	9.14	0.06	0.03	0.01	0.082	0.102
860 - 870	0.051	2.52	0.04	0.42	0.07	0.082	1110 - 1110	0.082	2.91	0.04	0.10	0.08	0.082	0.102
	0.138	1.75	0.06	0.20	0.20	0.102	0.102	0.126	2.52	0.06	0.37	0.12	0.082	0.102
							1110 - 1120	0.074	0.23	0.01	2.82	+	0.082	0.102
								0.061	0.25	0.07	61.82	25.92	0.102	0.102

[†] δ represents an upper limit and no uncertainty is given.[‡] The α_L^0 values were determined from the 810-800 cm^{-1} region and used for the other intervals.

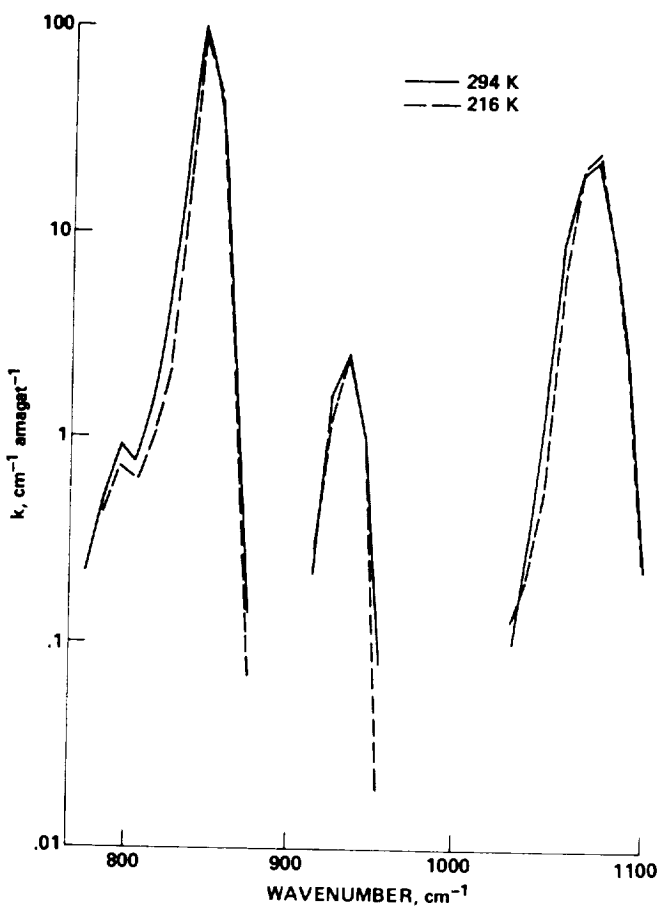


Fig. 1. The mean absorption coefficient, k , for freon 11 in the $770\text{--}1120\text{ cm}^{-1}$ region at 294 and 216°K .

profile was incorporated into the model was convergence achieved. The pressure domain of the data, 7×10^{-6} to 3×10^{-4} atm, necessitated the use of the Voigt profile with the Doppler halfwidth of $6 \times 10^{-4}\text{ cm}^{-1}$ as the dominant term. Except for the $810\text{--}880\text{ cm}^{-1}$ region of the spectrum, where k is the largest, we were unable to determine a Lorentz halfwidth. For this region, however, we found

$$\alpha_L^0 = \begin{cases} 0.08 \pm 0.01\text{ cm}^{-1}/\text{atm} & \text{at } 294^\circ\text{K}, \\ 0.10 \pm 0.04\text{ cm}^{-1}/\text{atm} & \text{at } 216^\circ\text{K}. \end{cases}$$

These values were used for the Lorentz broadening coefficient in the band model in order to calculate the mean absorption coefficient and the mean line spacing for all other intervals. Over the pressure range of the available data, the model is insensitive to the Lorentz broadening coefficient. For the $810\text{--}880\text{ cm}^{-1}$ region k changes by less than 6% as α_L^0 approaches zero. Because there was no significant difference detected when N_2 was added to the CFCl_3 ,⁵ we did not attempt to determine the nitrogen broadening coefficient.

For a few of the intervals, the fitting routine was unable to converge upon a value for the mean line spacing. In these cases the value of δ given in Table 1 is believed to represent an upper limit for the mean line spacing and therefore no uncertainty is given. For all intervals where absorption was observed, a value for the mean absorption coefficient, k , was determined. All the random errors in the laboratory data are reflected in the uncertainties (sigma) of the parameters listed in Table 1. If there are any systematic errors in the data, they must be factored into the results.

The band intensities were determined using Eq. (7) based on the absorption coefficients for the 10 cm^{-1} intervals. The results are presented in Table 2. There is as much as a 6% difference between these intensities and those derived from the broad intervals. It was found, for the

Table 2. Absolute intensities, S_v^o ($\text{cm}^{-1}/\text{cm-amagat}$),[†] of the i.r. bands of CFCl_3 (freon 11) in the 8-12 μm region.

Interval cm^{-1}	Temperature $^{\circ}\text{K}$	S_v^o ($\text{cm}^{-1}/\text{cm-amagat}$)	
		Previous Work (ref.)	Band Model
760-810	294	20.8 ± 3.6 (5)	24.0 ± 1.9
	216	11.2 ± 3.1 (5)	21.7 ± 7.2
810-880	294	1688 ± 49 (1) 1669 ± 135 (2) 1876 ± 281 (3) 1701 ± 48 (5)	1734 ± 13
	216	1556 ± 57 (5)	1641 ± 21
910-960	294	54.7 ± 2.7 (5)	55.5 ± 1.8
	216	49.2 ± 1.7 (5)	51.0 ± 1.2
1030-1120	294	698 ± 40 (1) 781 ± 67 (2) 576 (4) 645 ± 15 (5)	650.0 ± 3.5
	216	624 ± 17 (5)	638.1 ± 3.2

[†] atm_{stp} is taken as equivalent to amagat

810-880 cm^{-1} region, that as the interval widths were narrowed, the intensity converged to the sum from the 10 cm^{-1} intervals. The intensity derived from the 10 cm^{-1} intervals was well within the error limits for the summation based upon 20 cm^{-1} intervals. Consequently, it was felt that the intensity derived from intervals narrower than 10 cm^{-1} would be essentially the same as those reported in this work. This may be an artifact of replacing an integral with a finite sum in Eq. (7).

4. DISCUSSION AND CONCLUSION

The band model calculations accurately predict the laboratory observations, as evidenced by the low values of χ^2 in Table 1. Except for the very weak region, 760-810 cm^{-1} , at 216 $^{\circ}\text{K}$ the agreement with the measured intensity values listed in Table 2 is excellent. The agreement can also be seen in Fig. 2 where the synthetic spectrum is superimposed upon an actual laboratory observation. It was determined that the placement of the intervals did not significantly effect the results for the integrated band intensities.

The model predicts the measured transmission such that the residual $|\bar{T}_{\text{obs}} - \bar{T}_{\text{calc}}|$, is less than 0.005 in 90% of the cases and in no instance is the residual greater than 0.02. Having a model that is in excellent agreement with observations warrants a deeper examination of its parameters.

A comparison of the laboratory data and the band model calculations is displayed in Figs. 3 and 4. It can be seen from these curves that as kpl increases, the value of the mean line spacing has more influence on transmission. For different regions of the 810-880 cm^{-1} complex, when $kpl = 1$ the range of mean line spacings affects the transmission by as much as 10% (\bar{T} is near 50% at this point). We do not know of any measurements of the mean line spacing for CFCl_3 . However, Jennings¹¹ has measured freon 12 (CF_2Cl_2) with 10^{-4} cm^{-1} resolution and has been unable to find any single isolated lines for this lighter molecule. His results are consistent with the very small values of the mean line spacing derived by this model.

The other interesting parameter in the model is the Lorentz halfwidth, α_L^0 . Despite a less than ideal set of laboratory conditions, we have derived a single value for both 294 $^{\circ}\text{K}$ and 216 $^{\circ}\text{K}$. It is generally accepted that α_L^0 is proportional to $(T)^{-1/2}$, with which our values are consistent, e.g.

$$\frac{\alpha_L^0(294^{\circ}\text{K})}{\alpha_L^0(216^{\circ}\text{K})} = 0.8 \pm 0.3 \quad [\sqrt{(216/294)} = 0.86].$$

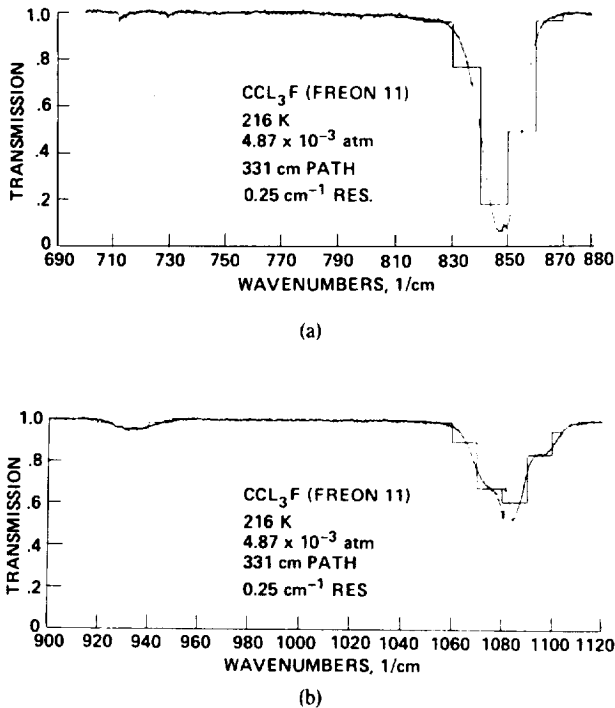


Fig. 2. Spectrum of freon 11 in the 8-12 μm region at 216°K with the synthetic spectrum derived from a band model superimposed.

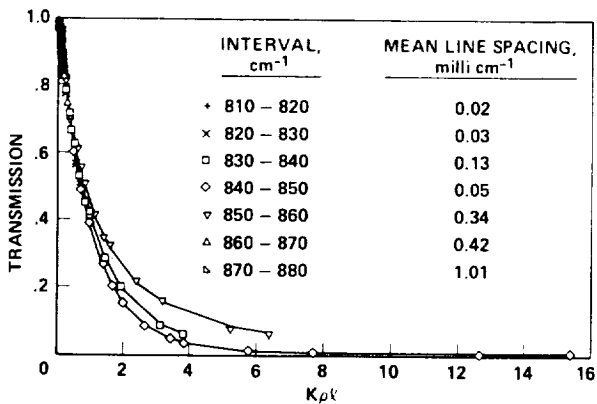


Fig. 3. Comparison of laboratory data and band-model calculations for freon 11 in the 810-880 cm^{-1} region at 294°K.

The similarity of transmission as a function of kpl for the 10 cm^{-1} intervals covering the band centers at 847 and 1085 cm^{-1} can be seen in Fig. 5. These two intervals exhibit the same behavior for both the room temperature and stratospheric temperature data. The small temperature dependence combined with the large absorption coefficients for these intervals should make them ideal candidates for stratospheric freon 11 abundance determination. Because these are 10 cm^{-1} intervals, low resolution experiments could be employed to take advantage of the results presented in this work. Band model parameters could be derived for intervals of higher resolution (0.25 cm^{-1} maximum) with the current data, if required.

This model compares directly with the laboratory measurements of Nanes *et al.*⁵ over a range of 4000 kpl . With the extremely small mean line spacings found it seems that the band model could be applied to intervals of much higher resolution. It is hoped that this model will prove useful in atmospheric calculations.

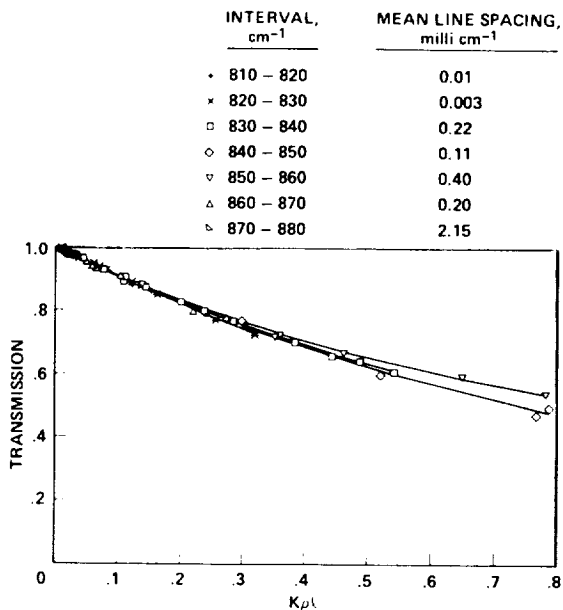


Fig. 4. Comparison of laboratory data and band-model calculations for freon 11 in the $810-880 \text{ cm}^{-1}$ region at 216°K .

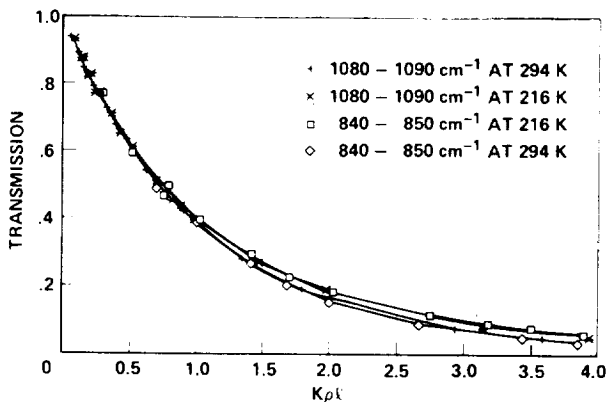


Fig. 5. Temperature dependence of band centers at 847 and 1085 cm^{-1} of freon 11.

Acknowledgements—The authors wish to thank M. Liu and R. Kosowski for their untiring efforts in the data reduction.

REFERENCES

1. P. Varnasi and F. K. Ko, *JQSRT* **17**, 385 (1977).
2. J. Herranz, R. de la Cierva, and J. Morcillo, *Annales Real Soc. Espan. Fis. Quim. (Madrid)* **A55**, 69 (1959). Quoted in W. B. Person, S. K. Rudys, and J. H. Newton, *J. Phys. Chem.* **79**, 2525 (1975).
3. A. Goldman, F. S. Bonomo, and D. G. Murcay, *Ap. Op.* **15**, 2305 (1976).
4. P. Jouve, *C. R. Acad. Sci., Paris* **B263**, 155 (1966).
5. R. Nanes, P. M. Silvaggio, and R. W. Boese, *JQSRT* **23**, 211 (1980).
6. R. M. Goody, *Atmospheric Radiation—I. Theoretical Basis*, p. 122. Clarendon Press, Oxford (1964).
7. S. S. Penner, *Quantitative Molecular Spectroscopy and Gas Emissivities*, p. 32. Addison-Wesley, Reading, Mass. (1959).
8. J. H. Pierlussi, P. C. Vanderwood, and R. B. Gomez, *JQSRT* **18**, 555 (1977).
9. C. de Boor, *Mathematical Software* (Edited by J. R. Rice), Chap. 7. Academic Press, New York (1971).
10. P. R. Bevington, *Data Reduction and Error Analysis for the Physical Sciences*, p. 204. McGraw-Hill, New York (1969).
11. D. E. Jennings, *Geophys. Res. Lett.* **5**, 241 (1978).